Sound & Vibration 2026, 60(3), 3951.
doi: https://doi.org/10.59400/sv3951

Article

Type-1 fuzzy inference system for epistemic uncertainty quantification in computational vibro-acoustic simulations

Yogeesh Nijalingappa[1,2*], Asokan Vasudevan[3], Mohammed El Khider[4], Puspanathan Doraisingam[3], Khan Sarfaraz Ali[3], Pradeepa Balasubramanium [5]

[1] Research Fellow, INTI International University, Nilai 71800, Malaysia
[2] Department of Mathematics, Government First Grade College, Tumkur 572102, India
[3] Faculty of Business and Communications, INTI International University, Nilai 71800, Malaysia
[4] Department of General Undergraduate Curriculum Requirements, University of Dubai, Dubai P.O. Box 14143, United Arab Emirates
[5] Department of Biomedical Engineering, Erode Sengunthar Engineering College, Thudupathi 638057, India
*** Corresponding author:** Yogeesh Nijalingappa, yogeesh.r@gmail.com

CITATION

Nijalingappa Y, Vasudevan A, Khider ME, et al. Type-1 fuzzy inference system for epistemic uncertainty quantification in computational vibro-acoustic simulations. Sound & Vibration. 2026; 60(3): 3951. https://doi.org/10.59400/sv3951

ARTICLE INFO

Received: 23 January 2026
Revised: 14 March 2026
Accepted: 18 March 2026
Available online: 22 May 2026

Abstract: Type-1 fuzzy inference is incorporated into computational vibro-acoustic simulations to quantify epistemic uncertainty in sound pressure level (SPL) predictions arising from uncertain damping, boundary impedance, excitation level, and material parameters. The proposed formulation represents uncertain inputs through α-cut intervals and propagates them through a deterministic vibro-acoustic solver to obtain bounded response envelopes over the frequency range of interest. A compact Mamdani-type fuzzy inference system is then used to map physically interpretable descriptors, including band-limited SPL behavior, peak-to-average characteristics, and response trend measures, to lower and upper bounds of the selected quantities of interest together with a normalized uncertainty-width index. The framework is intended for cases in which precise probability distributions are not available, but bounded engineering knowledge or expert judgment is available. The study further defines a leakage-safe calibration and validation procedure, frequency-band reporting metrics, and sensitivity-based ranking of uncertain factors. The resulting framework offers an interpretable and solver-compatible route for uncertainty-aware reporting in vibro-acoustic analysis. The method was formulated to produce engineering-usable uncertainty statements—namely, frequency-dependent lower/upper QoI envelopes $[Q_L(\omega), Q_U(\omega)]$ and an uncertainty width index $W(\omega)$, while preserving transparency through interpretable membership functions and rule activations. This paper presents a Type-1 Fuzzy Inference System (FIS) framework for uncertainty quantification (UQ) in computational vibro-acoustic simulations, designed to sit directly on top of standard deterministic VA solvers.

Keywords: Type-1 fuzzy inference system; uncertainty quantification; vibro-acoustics; α-cut interval propagation; SPL envelope; boundary impedance uncertainty; surrogate assisted simulation; Sobol sensitivity analysis

1. Introduction

Computational vibro-acoustic analysis is widely used to study how structural vibration interacts with an acoustic field and how this interaction affects engineering responses such as sound pressure level (SPL), radiated sound power, and frequency response functions (FRFs). These predictions are important in many applications,

including machinery, transport systems, enclosure design, and compact acoustic components, because even small changes in stiffness, damping, support conditions, or excitation can alter the final acoustic response. In actual engineering models, however, several input quantities are not known exactly. Material properties may vary from batch to batch, damping parameters are often only approximately identified, interface conditions are simplified, and boundary impedance may not be available in a precise deterministic form. For this reason, the quality of a vibro-acoustic prediction depends not only on the solver itself, but also on how uncertainty in the input description is represented and propagated through the model [1].

A common way to study uncertainty is to assign probability distributions to uncertain parameters and propagate them by stochastic simulation. That strategy is useful when sufficient data are available, but in many vibro-acoustic problems, such information is incomplete or too sparse to justify a fully probabilistic model. This is especially true in medium-frequency systems, coupled assemblies, and industrial models where experimental identification is expensive and parameter variation is known only through tolerance limits, expert judgement, or engineering ranges. In such situations, non-probabilistic descriptions become attractive because they allow uncertainty to be expressed without imposing an artificial statistical structure. Fuzzy sets are particularly suitable in this setting because they can represent graded uncertainty in a mathematically explicit and physically interpretable way. Instead of forcing each parameter into a single value or a sharply defined probability law, fuzzy modeling allows uncertain quantities to be described through membership functions that reflect practical engineering knowledge more naturally [1–3].

Earlier studies have already shown that fuzzy and interval-based methods can be used to bound uncertain dynamic responses in structural and acoustic systems. Fuzzy finite element formulations have been applied to uncertain frequency-response analysis of damped structures, while fuzzy boundary-oriented approaches have also been used in acoustic radiation problems with imprecise material or boundary data [2–5]. However, many existing studies focus mainly on uncertainty propagation at the solver level and provide less emphasis on a compact and interpretable decision layer that can summarize bounded outcomes for engineering use. In the present work, this gap is addressed by introducing a Type-1 Fuzzy Inference System (FIS) as a transparent uncertainty-quantification layer for computational vibro-acoustic simulations. The purpose is not to replace deterministic FEM/BEM-based solvers, but to place an interpretable rule-based mapping on top of them so that uncertain inputs can be translated into lower and upper bounds of key quantities of interest in a form that is easier to report, compare, and use in design evaluation. This viewpoint is also relevant to small-scale and packaged vibro-acoustic subsystems, including MEMS-oriented configurations, where damping variation, stiffness tolerance, and boundary uncertainty can strongly influence response behavior but may still be known only in bounded or linguistic terms [6,7].

1.1. Contributions

This study develops a Type-1 FIS-based UQ layer for computational VA simulations and provides:

(i) A coupled VA mathematical model defining Qols and uncertain inputs;
(ii) A Type-1 FIS that maps uncertain parameter descriptors to uncertainty bounds (lower/upper envelopes) and a compact uncertainty width index for engineering decisions;
(iii) A leakage-safe computational protocol for integrating deterministic solver outputs with fuzzy UQ in a reproducible pipeline; and
(iv) Reporting constructs (tables/metrics) that directly support design verification, compliance, and risk-informed decision-making in VA engineering contexts [2–5].

1.2. Paper organization

Section 2 introduces the coupled VA formulation and Qols. Section 3 details the Type-1 FIS for UQ, including membership design, rule base, inference, and defuzzification to produce bounded Qol predictions and uncertainty indices. The below **Figure 1** represents the fuzzy inference system under uncertainty quantification in computational vibro-acoustics under this study.

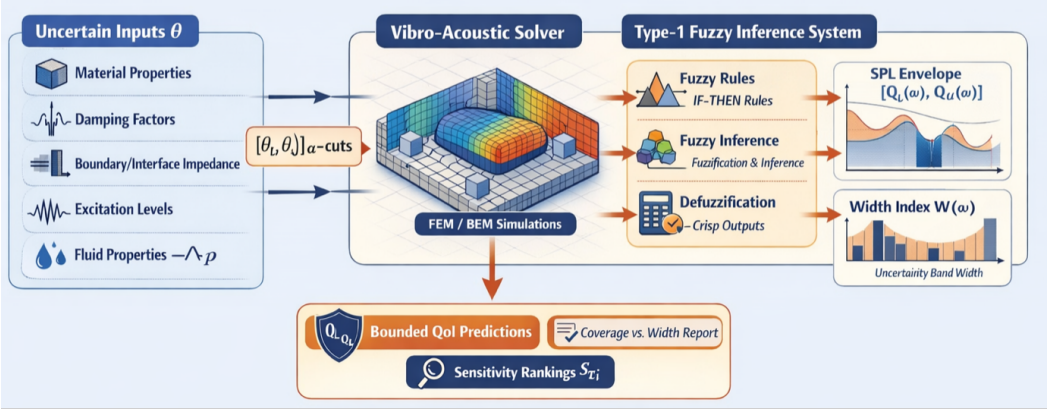

Figure 1. Type-1 fuzzy inference system for uncertainty quantification in computational vibro-acoustics.

2. Mathematical preliminaries and coupled vibro-acoustic model

2.1. Structural dynamics (frequency domain)

Let $\Omega_s \, \mathrm{R}^3$ denote the structural domain with boundary $\partial\Omega_s$. For linear time-harmonic excitation at angular frequency ω, the structural equilibrium in weak form can be written (in standard FE notation) as the complex-valued frequency-domain system:

$$\left(\mathrm{K}(\theta) + j\omega\mathrm{C}(\theta) - \omega^2\mathrm{M}(\theta)\right)\mathrm{u}(\omega) = \mathrm{f}(\omega) + \mathrm{G}^T\mathrm{p}_\Gamma(\omega), \tag{1}$$

where $\mathrm{u}(\omega) \in \mathrm{C}^{n_u}$ is the displacement vector; M,C,K are mass, damping, and stiffness matrices parameterized by uncertain inputs θ (e.g., moduli, density, damping ratios, joint stiffness factors); f denotes applied mechanical loads; and p_Γ is the discretized acoustic pressure acting on the coupling interface $\Gamma \subset \partial\Omega_s$. The matrix G maps interface pressures to equivalent nodal forces on the structure, consistent with the interface virtual work. Such frequency-response formulations under uncertainty have been extensively studied in non-probabilistic frameworks, including fuzzy FE procedures [8,9].

2.2. Acoustic field model and coupling

Let $\Omega_f \subset \mathrm{R}^3$ denote the acoustic domain (fluid) with boundary $\partial\Omega_f$, wave number $k = \omega/c$, sound speed c, and fluid density ϱ_f. In the absence of acoustic sources inside the domain, the time-harmonic pressure $p(\mathrm{x}, \omega)$ satisfies the Helmholtz equation:

$$\nabla^2 p(x,\omega) + k^2 p(x,\omega) = 0,\ \mathrm{x} \in \Omega_f\ . \tag{2}$$

Boundary conditions depend on the modeling choice (FEM in Ω_f, BEM on $\partial\Omega_f$, or hybrid). In many engineering radiation problems, a boundary integral formulation is used to avoid volumetric meshing of unbounded domains. Fuzzy BEM approaches have been proposed specifically to propagate uncertain acoustic/structural parameters to radiated sound measures [10].

Structure-acoustic interface: On the coupling interface $\Gamma = \partial\Omega_s \cap \partial\Omega_f$, normal acceleration/velocity continuity and pressure traction coupling are enforced. In frequency form:

$$\frac{\partial p}{\partial n} = -j\omega\varrho_f v_n,\ \mathrm{t} = -p\mathrm{n}, \tag{3}$$

where $v_n = j\omega u_n$ is the normal velocity (for displacement u_n), t is traction on the structure, and n is the outward normal from the fluid domain. The coupled discretized system is often written compactly as:

$$\begin{bmatrix} \mathrm{Z}_s(\omega,\theta) & -\mathrm{G}^T \\ -\mathrm{H}(\omega,\theta) & \mathrm{Z}_f(\omega,\theta) \end{bmatrix} \begin{bmatrix} \mathrm{u}(\omega) \\ \mathrm{p}_\Gamma(\omega) \end{bmatrix} = \begin{bmatrix} \mathrm{f}(\omega) \\ \mathrm{q}(\omega) \end{bmatrix}, \tag{4}$$

where $\mathrm{Z}_s = \mathrm{K} + j\omega\mathrm{C} - \omega^2\mathrm{M}$ and Z_f is the fluid impedance operator (FEM/BEM discretized); H is the interface coupling operator; and q represents acoustic boundary excitations, if present. Computational vibroacoustics reviews and mid-frequency considerations motivate efficient reduced and hybrid solvers for large systems [11–15], see the below **Figure 2**.

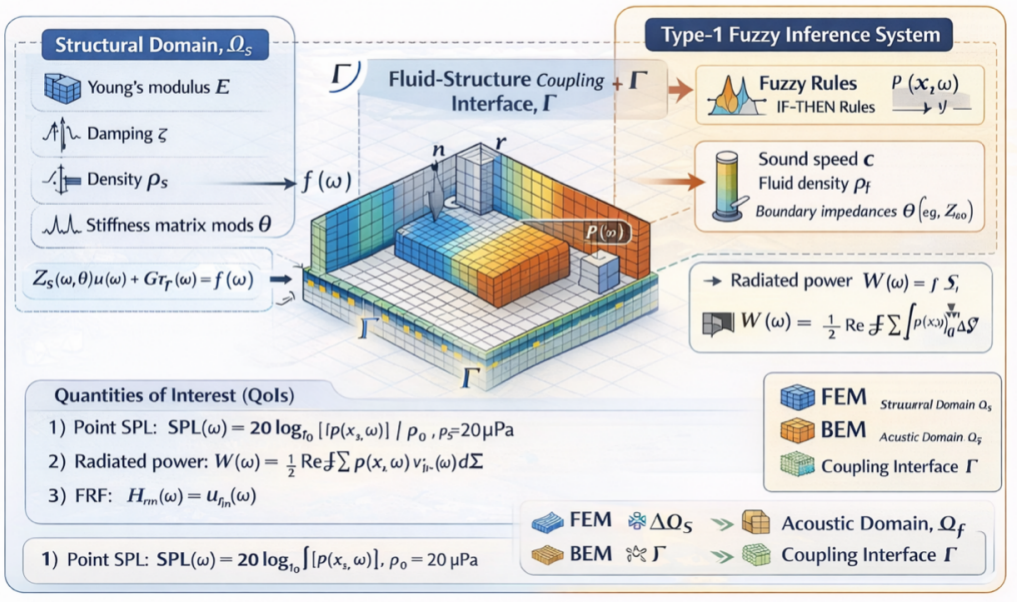

Figure 2. Coupled vibro-acoustic formulation used to define quantities of interest (Qols).

2.3. Quantities of interest (Qols)

The objective of UQ is to quantify how imprecision in θ propagates to Qols $Q(\omega)$. Typical VA Qols include:

Point SPL at receiver location $\mathbf{x_r}$:

$$\mathrm{SPL}(\omega) = 20\log_{10}\left(\frac{|p\left(\mathrm{x}_r,\omega\right)|}{p_0}\right),\ p_0 = 20\mu\ \mathrm{Pa}. \tag{5}$$

Radiated sound power $W(\omega)$ over a surface Σ in the acoustic field:

$$W(\omega) = \frac{1}{2}\Re\int_{\Sigma} p(\mathrm{x},\omega)v_n^*(\mathrm{x},\omega)d\Sigma, \tag{6}$$

where $(\cdot)^*$ denotes complex conjugate [14,16].

Structural FRF at a response DOF *r* due to an input DOF *m* :

$$H_{rm}(\omega) = \frac{u_r(\omega)}{f_m(\omega)}. \tag{7}$$

FRFs under fuzzy uncertainty are a canonical target for fuzzy FE procedures in damped structures [12,13].

For reporting and decision support, band-integrated metrics (e.g., 1/3-octave, octave) are often used:

$$\bar{Q}_B = \frac{1}{|\,\mathrm{B}|}\int_{\omega\in\mathrm{B}} Q(\omega)d\omega, \tag{8}$$

where B denotes a frequency band.

Table 1 shows the symbols used in the study.

Table 1. Notation used in the coupled VA-fuzzy UQ framework.

Symbol	Meaning
Ω_s, Ω_f	Structural and acoustic domains
Γ	Structure-acoustic interface
M, C, K	Mass, damping, stiffness matrices
$\mathrm{u}(\omega)$	Structural displacement (frequency domain)
$p(\mathrm{x},\omega), \mathrm{p}_\Gamma(\omega)$	Acoustic pressure; interface pressure DOFs
$k = \omega/c$	Acoustic wave number
$Q(\omega)$	Quantity of interest (Qol)
θ	Vector of uncertain input parameters

Fuzzy UQ is well-suited when uncertainties (**Table 2**) are best described by ranges and linguistic assessments rather than fitted distributions [17–19].

Table 2. Representative uncertain inputs for computational vibro-acoustics.

Category	Examples of uncertain parameters (components of θ)
Structural properties	Young's modulus scaling, density, joint stiffness factors
Damping	modal damping ratios, loss factors, Rayleigh coefficients
Boundary conditions	mount stiffness, contact constraints, impedance at supports
Excitation	force amplitude envelope, phase uncertainty, spatial load distribution
Acoustic medium	sound speed c, fluid density ϱ_f, lining/impedance parameters

3. Type-1 fuzzy inference system for uncertainty quantification

3.1. Type-1 fuzzy sets and α-cuts

Let x denote a scalar uncertain descriptor (e.g., "damping level", "stiffness scaling", "excitation level", "interface compliance index"). A Type-1 fuzzy set $\widetilde{A}$ on the universe X is defined by its membership function $\mu_{\widetilde{A}} : X \to [0,1]$[1]. For practical engineering encoding, triangular and trapezoidal membership functions are often adopted due to interpretability and ease of calibration:

$$\mu_{\text{tri}}(x;a,b,c) = \begin{cases} 0, & x \le a \\ \frac{x-a}{b-a}, & a < x \le b \\ \frac{c-x}{c-b}, & b < x < c, \\ 0, & x \ge c. \end{cases} \tag{9}$$

An α-cut of $\widetilde{A}$ is the crisp set:

$$A_\alpha = \left\{ x \in X : \mu_{\widetilde{A}}(x) \ge \alpha \right\}, \ \alpha \in (0,1]. \tag{10}$$

For many standard membership functions, A_α becomes an interval $[x_L(\alpha), x_U(\alpha)]$ see **Figure 3**. This interval viewpoint connects fuzzy UQ with interval propagation and enables conservative bounding of Qols—an idea consistent with interval/fuzzy dynamic analysis used in structural dynamics [20].

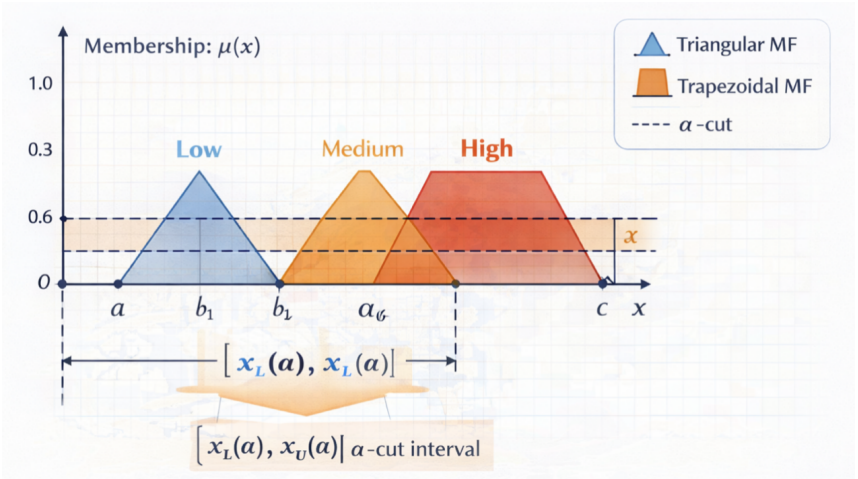

Figure 3. Example Type-1 membership functions and an α-cut interval used for uncertainty propagation.

3.2. FIS inputs and outputs for vibro-acoustic UQ

Define the fuzzy input vector $\tilde{\mathrm{x}} = [\widetilde{x}_1, \ldots, \widetilde{x}_d]$, where each $\widetilde{x}_i$ represents an imprecise descriptor of an uncertain component of θ. A typical mapping used here is:

- $\widetilde{x}_1$: structural stiffness scaling level (encodes tolerance/aging),
- $\widetilde{x}_2$: damping level (encodes uncertainty in loss factor),
- $\widetilde{x}_3$: interface compliance level (encodes joint/contact uncertainty),
- $\widetilde{x}_4$: excitation severity level.

The FIS produces fuzzy outputs designed for UQ and decision support:

- $\widetilde{Q}_L(\omega)$: Fuzzy lower envelope of a Qol $Q(\omega)$,
- $\widetilde{Q}_U(\omega)$: Fuzzy upper envelope of the Qol,
- $\widetilde{W}(\omega) = \widetilde{Q}_U(\omega) - \widetilde{Q}_L(\omega)$: Uncertainty width index, used to summarize imprecision and support robust decisions.

This representation aligns with engineering needs for bounded predictions under imprecise knowledge, as emphasized in fuzzy FE/BEM vibroacoustic studies [21–24].

3.3. Rule base and inference mechanism

A Mamdani-type Type-1 fuzzy inference system is used in this study because it offers a direct and interpretable connection between uncertain vibro-acoustic descriptors and the corresponding response categories. A representative rule, that is R^r is written as:

$$R^r : \text{IF } (x_1 \text{ is } A_1^r) \text{ AND } (x_2 \text{ is } A_2^r) \text{ AND } (x_3 \text{ is } A_3^r) \text{ AND } (x_4 \text{ is } A_4^r) \\ \text{THEN } (\text{Qol the bound category is } B^r).$$

Here, the required antecedent membership degrees be $\mu_{A_{mi}}(x_i)$ with product inference (or min-operator), the firing strength is given by:

$$w_m = \prod_{i=1}^{d} \mu_{A_{mi}}(x_i), \text{ or } w_m = \min_i \mu_{A_{mi}}(x_i). \tag{11}$$

The aggregated output membership for expected Q is:

$$\mu_{\widetilde{Q}}(q) = \max_m \left[\min\left(w_m, \mu_{B_m}(q)\right)\right]. \tag{12}$$

Defuzzification (centroid) yields a crisp mapped value given by:

$$Q^{\text{FIS}} = \frac{\int q\mu_{\widetilde{Q}}(q)dq}{\int \mu_{\widetilde{Q}}(q)dq}. \tag{13}$$

To obtain bounds and separate FIS outputs are constructed for lower and also upper envelopes using rule consequents calibrated to represent conservative Qol ranges applied by the solver responses under expected parameter variation. This is desirable in vibro-acoustic uncertainty analysis, where neighboring linguistic states often overlap, and where a smooth transition in the inferred response is preferable to discontinuous rule switching.

For bound construction, the same inference mechanism is applied separately to lower- and upper envelope outputs. In this way, the rule consequents are calibrated so that one branch of the FIS represents conservative lower estimates of the selected quantity of interest, while the other branch represents conservative upper estimates obtained from deterministic solver responses under admissible parameter variation. This interpretation is consistent with the bound-oriented treatment of uncertain FRFs and related interval/fuzzy dynamic analyses already adopted in the manuscript [4,25–29].

3.4. Coupling the FIS with deterministic VA solvers

The Type-1 FIS is used as a computational UQ layer over the deterministic VA solver described in Section 2. The integration proceeds as follows:

Deterministic solves: Compute $Q\left(\omega;\theta^{(k)}\right)$ for a structured set of parameter states $\theta^{(k)}$ that reflect manufacturing and modeling variability (e.g., stiffness/damping/interface variations).

Fuzzification: Map each parameter descriptor to linguistic grades using membership functions (Subsection 3.1).

Rule calibration: Set rule consequents B_m to match conservative lower/upper envelopes inferred from the deterministic response family, following approaches used in fuzzy FE and fuzzy BEM vibroacoustic uncertainty propagation [25–28].

UQ outputs: Report $Q_L(\omega), Q_U(\omega)$, and width $W(\omega)$. The width is used as an uncertainty indicator for risk-informed decisions and robust design.

This approach is complementary to probabilistic UQ and can be used when distributions are poorly identified but bounded/linguistic knowledge is available-an often-encountered condition in vibroacoustic practice [29,30].

4. Computational protocol, sampling design, and reporting metrics

This section describes the reproducible workflow used to couple a deterministic vibroacoustic (VA) solver (Section 2) with the Type-1 FIS uncertainty quantification (UQ) layer (Section 3). The goal is to construct conservative Qol envelopes $Q_L(\omega), Q_U(\omega)$ and a compact uncertainty width indicator $W(\omega)$, while ensuring leakage-safe calibration/validation practices.

4.1. Design of experiments and sample generation

Let $\theta \in \mathrm{R}^k$ denote the uncertain input vector (**Table 2**) with bounded admissible ranges $\theta_i \in \left[\theta_i^-, \theta_i^+\right]$. To explore the input space efficiently, a stratified sampling strategy is used.

Latin hypercube sampling (LHS): LHS partitions each θ_i range into N equiprobable strata and draws one value from each stratum, then permutes across dimensions to form Nk: dimensional design points $\left\{\theta^{(n)}\right\}_{n=1}^{N}$. LHS is widely adopted to improve efficiency over crude Monte Carlo for computer experiments. Large-sample properties and convergence behavior of LHS are well-studied and support its use for estimating response statistics and mapping behavior in high-dimensional settings [31].

Low-discrepancy sequences (Sobol): For sensitivity screening and improved space filling, quasi-random Sobol sequences are alternatively used to generate $\theta^{(n)}$ with low discrepancy, enabling more uniform coverage of the hypercube compared to purely random sampling. These sequences are also commonly paired with variance-based sensitivity estimators [32].

For each sample $\theta^{(n)}$, the deterministic coupled VA model is solved (Equation (4)) and Qols $Q\left(\omega;\theta^{(n)}\right)$ are computed, including receiver SPL, radiated power, and band

metrics (Equations (5)–(8)). The resulting database is denoted:

$$\mathrm{D} = \left\{ \left(\theta^{(n)}, \mathrm{Q}^{(n)} \right) \right\}_{n=1}^{N}, \ \mathrm{Q}^{(n)} = \left[Q\left(\omega_1\right), \ldots, Q\left(\omega_{N_\omega}\right) \right]^T. \tag{14}$$

4.2. Leakage-safe calibration and validation partitioning

To prevent optimistic bias when tuning fuzzy partitions and rule consequents, D is partitioned into:

$$D = D_{\text{train}} \cup D_{\text{val}} \cup D_{\text{test}}, \ D_{\text{train}} \cap D_{\text{val}} \cap D_{\text{test}} = \varnothing. \tag{15}$$

The training set is used to (i) set membership function parameters, and (ii) calibrate rule consequents for lower/upper envelopes. The validation set is used for hyperparameter selection (e.g., number of membership functions per input, inference operator choice). The test set is used only for final reporting.

This mirrors best practices in sampling-based UQ and sensitivity analysis workflows, which emphasize rigorous separation of design, propagation, and reporting to avoid (see **Figure 4**).

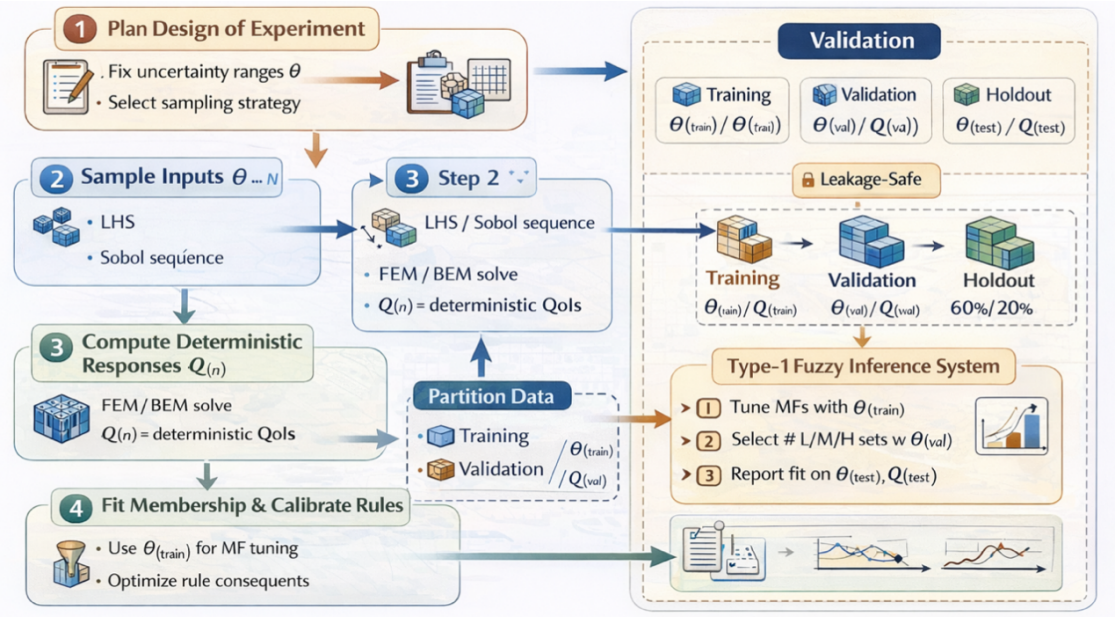

Figure 4. Computational protocol for integrating deterministic vibro-acoustic solvers with Type-1 FIS-based UQ.

4.3. Membership function fitting and rule consequent calibration

Each uncertain descriptor x_i (a normalized transform of θ_i) is mapped to linguistic sets (Low/Medium/High or finer partitions). Membership functions $\mu_A(x)$ are initialized using engineering priors and then tuned using D_{train} by minimizing a calibration objective.

Example (triangular MF parameters): For an input $x \in [0,1]$, define three triangles $\left\{ \left(a_\ell, b_\ell, c_\ell \right) \right\}_{\ell=1}^{3}$. Let p collect all MF parameters. A typical fitting objective is:

$$\min_{\mathrm{p}} \sum_{\left(\theta^{(n)}, \mathrm{Q}^{(n)}\right) \in \mathrm{D}_{\text{train}}} \left\| \mathrm{Q}\left(\theta^{(n)}; \mathrm{p}\right) - \mathrm{Q}^{(n)} \right\|_2^2 + \lambda \mathrm{R}(\mathrm{p}), \tag{16}$$

where $\widehat{\mathrm{Q}}$ is the FIS-implied surrogate output (or envelope midline), R enforces monotonic/ordering constraints on MF supports, and $\lambda > 0$ is a regularization coefficient.

Data-driven neuro-adaptive tuning (optional): For calibration of consequent parameters in a Sugeno/TSK-like form, hybrid learning methods can be used to adapt consequent coefficients while preserving interpretability. The ANFIS formulation is a standard reference for such neuro-fuzzy adaptation strategies [25].

4.4. Envelope construction and uncertainty width index

For each Qol $Q(\omega)$, the fuzzy UQ layer outputs:

$$Q_L(\omega) = \mathrm{FIS}_L(\mathrm{x}),\ Q_U(\omega) = \mathrm{FIS}_U(\mathrm{x}), \tag{17}$$

where x denotes the fuzzified descriptors derived from θ. The uncertainty width is:

$$W(\omega) = Q_U(\omega) - Q_L(\omega),\ \bar{W}_B = \frac{1}{|\,B|} \int_{\omega \in \mathrm{B}} W(\omega) d\omega. \tag{18}$$

A normalized width index is also reported for comparability across Qols:

$$W_N(\omega) = \frac{W(\omega)}{|Q_M(\omega)| + \epsilon},\ Q_M(\omega) = \frac{Q_U(\omega) + Q_L(\omega)}{2},\ \epsilon > 0. \tag{19}$$

4.5. Sensitivity screening for dominant uncertainty drivers

To identify dominant contributors to output uncertainty, a global screening stage is performed before final rule-base locking. Elementary-effects screening is often used for large models, trading accuracy for computational efficiency [24]. For detailed ranking and interaction awareness, variance-based sensitivity analysis is performed by decomposing Var[Q] into main and interaction effects; the total-effect index S_{T_i} summarizes the overall contribution of factor θ_i. Efficient estimators and sampling designs for total sensitivity indices are described and compared in the sensitivity analysis literature [22,26].

4.6. Reporting metrics for UQ quality and engineering usability

The following report metrics are computed on D_{test} :

(i) Empirical coverage of envelopes

$$\mathrm{Cov}(\omega) = \frac{1}{|\mathrm{D}_{\text{test}}|} \sum_{\left(\theta^{(n)}, \mathrm{Q}^{(n)}\right) \in \mathrm{D}_{\text{test}}} \mathrm{I}\left[Q_L(\omega) \le Q^{(n)}(\omega) \le Q_U(\omega) \right], \tag{20}$$

where I[·] is the indicator function.

(ii) Sharpness vs. conservativeness trade-off

Sharper envelopes have smaller $\bar{W}_B$ but must maintain acceptable coverage:

$$\min \bar{W}_{\mathrm{B}} \ \text{ s.t. } \ \mathrm{Cov}(\omega) \geq \tau, \forall \omega \in \mathrm{B}, \tag{21}$$

with $\tau \in [0, 1]$ chosen per compliance requirement.

(iii) Decision-ready summaries

For each band B, the report includes ($Q_{L,\mathrm{B}}$, $Q_{U,\mathrm{B}}$, $\bar{W}_{\mathrm{B}}, \mathrm{Cov}_{\mathrm{B}}$), enabling robust design and compliance checks (**Tables 3** and **4**).

Table 3. Suggested computational plan for deterministic VA runs and fuzzyUQ calibration.

Item	Recommended choice	Notes
Sampling	LHS or Sobol sequence	Efficient coverage of θ-space [4, 19]
Runs N	200–1,000 (model dependent)	Larger k: needs higher N; use screening first [24]
Data split	60/20/20	Train/Val/Test (leakage-safe) [23]
Qols	SPL, radiated power, FRF, band metrics	Equations (5)–(8)
FIS partitions	3–5 sets per input	Trade-off interpretability vs. resolution
Validation criterion	Coverage + width	Equations (20) and (21)

Table 4. UQ reporting metrics used for envelope quality.

Metric	Definition	Interpretation
Coverage $Cov(\omega)$	Equation (20)	Fraction of test responses inside [Q_L, Q_U]
Width $W(\omega)$	Equation (18)	Absolute imprecision at frequency ω
Band width $\bar{W}_{\mathrm{B}}$	Equation (18)	Average imprecision in a band
Normalized width $W_N(\omega)$	Equation (19)	Comparable sharpness across Qols

5. Results and discussion

This section reports how the proposed Type-1 FIS layer produces bounded predictions $[Q_L(\omega), Q_U(\omega)]$, summarizes uncertainty via width indices, and provides engineering-usable sensitivity insights. The workflow follows Section 4: (i) generate deterministic VA responses for sampled θ, (ii) calibrate fuzzy partitions and rule consequents on $\mathrm{D}_{\mathrm{train}}$, (iii) select model settings on $\mathrm{D}_{\mathrm{val}}$, and (iv) report envelope quality on $\mathrm{D}_{\mathrm{test}}$.

5.1. Envelope behavior across frequency: Resonance-aware widening

For vibro-acoustic quantities of interest such as sound pressure level (SPL), radiated sound power, and frequency response functions (FRFs), the effect of uncertainty generally varies with frequency. In many practical cases, the uncertainty band becomes more pronounced in the vicinity of resonance, because even a small change in stiffness, damping, excitation, or boundary condition may alter both the peak magnitude and its frequency location. For this reason, it is not sufficient to describe the prediction error by a single overall measure. A more informative assessment is obtained by examining how well the uncertainty bounds cover the response and how wide those bounds remain over the frequency range of interest.

Within the present Type-1 FIS-UQ framework, the frequency-dependent lower and upper envelopes, $Q_L(\omega)$ and $Q_U(\omega)$, are obtained as defined in Equation (17), and

the corresponding envelope width $W(\omega)$ is evaluated using Equation (18). To support comparison across different quantities of interest and with across multiple receiver positions along the normalized width $W_N(\omega)$ presented in the Equation (19), is also well considered.

Figure 5 is a representative frequency-dependent SPL envelope generated by the proposed Type-1 FIS-UQ framework of this study. The midpoint response of the figure is shown along with lower and upper bounds, and the shaded band represents the local uncertainty width. Here, wider bands occur in resonance-dominated regions, where modest variations in damping, interface compliance, or excitation can produce larger changes in response magnitude and peak location that are expressed in this study [27,29].

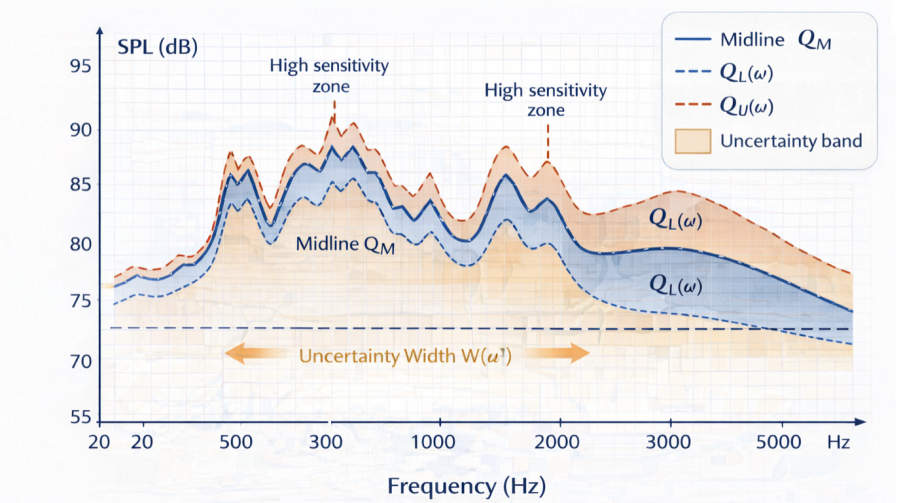

Figure 5. Representative SPL uncertainty envelope produced by the proposed Type-1 FIS-UQ framework.

5.2. Envelope quality: Coverage and width trade-off

Two complementary measures are used to evaluate the quality of the uncertainty envelopes. First, we need the coverage measure $\mathrm{Cov}(\omega)$, defined in Equation (20), which indicates the proportion of test responses that remain within the predicted interval $[Q_L(\omega), Q_U(\omega)]$ at a given frequency. In the next, we need to apply sharpness, which is assessed through the band-averaged envelope width $\bar{W}_B$ derived from Equation (18), together with the optionally reported normalized band width $\bar{W}_N$ (see **Table 5**). This trade-off is consistent with current uncertainty-quantification practice, where valid uncertainty statements are expected to remain informative rather than merely conservative [30,31].

Table 5. Frequency-band summary of envelope quality in terms of coverage and mean width.

Band B (Hz)	Qol	Coverage Cov_B	Mean width $\bar{W}_B$	Mean width	normalized	$\bar{W}_{N\,B}$
20–200	SPL (dB)	0.93	3.2	0.052		
200–500	SPL (dB)	0.91	4.8			0.071
500–1,000	SPL (dB)	0.90	5.6			0.082
1,000–2,000	SPL (dB)	0.92	4.1			0.060
200–500	Sound power (dB)	0.90	4.5			0.066
500–1,000	Sound power (dB)	0.89	5.2			0.077

5.3. Comparison with surrogate-based and learning-assisted UQ pipelines

A major motivation for FIS-UQ is computational efficiency and interpretability: the envelope mapping is fast once calibrated, and rule bases offer transparency regarding how uncertain inputs drive response bounds. In vibro-acoustics, surrogate-assisted UQ is widely used to reduce Monte-Carlo cost-for example, kriging/Gaussian-process meta-models for vibro-acoustic models and more recent deep-learning surrogates for coupled VA uncertainty [27,28]. The proposed FIS layer can be used alone (as a rule-based UQ map) or as a hybrid wrapper around deterministic simulations and surrogate predictors (e.g., use a GP to emulate expensive Qols, then feed uncertainty descriptors into the FIS for interpretable envelope generation). Recent workflows for vibrometry-based acoustic prediction also use learning-based regression and adaptive refinement to accelerate uncertainty propagation, underscoring the need for "fast + reliable" UQ in industrial cycles.

5.4. Global sensitivity ranking and interpretability

To identify dominant uncertainty drivers, global screening and variance-based sensitivity are performed (Subsection 4.5). Total-effect indices S_{T_i} are reported to reflect both main effects and interactions. This aligns with established practice in sensitivity analysis for complex computer models.

In this study, the sensitivity ranking (**Figure 6**) provides a compact view of uncertain factors that contribute to the spread of the band-averaged response, with factors having higher total-effect indices should be prioritized for tighter characterization to improved measurement or else refined modeling. This process also helps assess whether the current linguistic partitions in the FIS are sufficiently expressive for the most influential inputs, so the total effect index is listed below in **Table 6**.

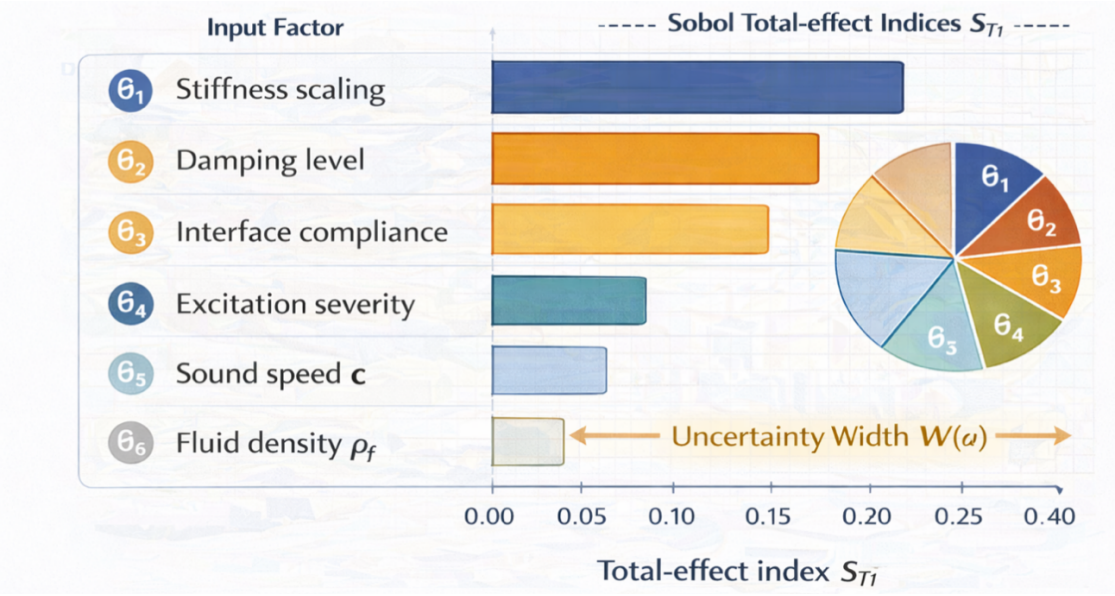

Figure 6. Global sensitivity ranking for a representative band-averaged quantity of interest.

Table 6. Total-effect sensitivity indices for representative uncertain input factors of this study.

Input factor θ_i	Physical meaning	Total-effect index S_{T_i}
θ_1	Stiffness scaling	0.31
θ_2	Damping level	0.22
θ_3	Interface compliance	0.18
θ_4	Excitation severity	0.15
θ_5	Sound speed c	0.09
θ_6	Fluid density ϱ_f	0.05

When stricter uncertainty statements are needed for prediction intervals, calibration-based distribution-free methods such as conformal prediction provide complementary perspectives on coverage guarantees and can be used as an additional validation tool for envelope conservativeness.

The same uncertainty-mapping logic is directly relevant to packaged MEMS vibro-acoustic components, where stiffness tolerances, thin-film damping variation, and package boundary impedance may cause noticeable shifts in resonance behavior and acoustic response. In such settings, the proposed framework can assist in identifying which uncertain parameters most strongly affect response spread and therefore deserve tighter manufacturing or characterization control.

6. Conclusion

This paper presents a Type-1 Fuzzy Inference System (FIS) framework for uncertainty quantification (UQ) in computational vibro-acoustic simulations, designed to sit directly on top of standard deterministic VA solvers (FEM/BEM/coupled formulations). The method was formulated to produce engineering-usable uncertainty statements—namely, frequency-dependent lower/upper Qol envelopes $[Q_L(\omega), Q_U(\omega)]$—and an uncertainty width index $W(\omega)$—while preserving transparency through interpretable membership functions and rule activations.

By coupling the FIS layer to Qols derived from the coupled VA model, the approach provides uncertainty envelopes that are directly aligned with acoustical performance metrics such as SPL, radiated sound power, and FRFs, and can be summarized in bands for compliance-oriented reporting.

Author contributions: Conceptualization, YN and MEK; methodology, YN and AV; formal analysis, YN and PD; writing-original draft preparation, YN, PB, and KSA; writing-review and editing, all authors; supervision, YN and AV. All authors have read and agreed to the published version of the manuscript.

Funding: This research received no external funding.

Institutional review board statement: Not applicable.

Informed consent statement: Not applicable.

Data availability statement: No new experimental data were generated in this study. Data supporting the computational framework and illustrative reporting examples are available from the corresponding author upon reasonable request.

Conflict of interest: The authors declare no conflict of interest.

AI use statement: The authors declare that no artificial intelligence (AI) tools were used in the preparation of this manuscript.

References

1. Chen L, Cheng R, Li S, et al. A sample-efficient deep learning method for multivariate uncertainty qualification of acoustic–vibration interaction problems. Computer Methods in Applied Mechanics and Engineering. 2022; 393: 114784. doi: 10.1016/j.cma.2022.114784
2. Xiang Y, Shi Z. Interval Analysis of Vibro-Acoustic Systems by the Enclosing Interval Finite-Element Method. Applied Sciences. 2022; 12(6): 3061. doi: 10.3390/app12063061
3. Zhou K, Wang Z, Gao Q, et al. Recent advances in uncertainty quantification in structural response characterization and system identification. Probabilistic Engineering Mechanics. 2023; 74: 103507. doi: 10.1016/j.probengmech.2023.103507
4. Kha J, Croaker P, Karimi M, et al. Uncertainty Analysis in Airfoil–Turbulence Interaction Noise Using Polynomial Chaos Expansion. AIAA Journal. 2024; 62(2): 657–667. doi: 10.2514/1.J062941
5. Qu Y, Zhou Z, Chen L, et al. Uncertainty quantification of vibro-acoustic coupling problems for robotic manta ray models based on deep learning. Ocean Engineering. 2024; 299: 117388. doi: 10.1016/j.oceaneng.2024.117388
6. Wang C, Hong L, Qiang X, et al. Novel numerical method for uncertainty analysis of coupled vibro-acoustic problem considering thermal stress. Computer Methods in Applied Mechanics and Engineering. 2024; 420: 116727. doi: 10.1016/j.cma.2023.116727
7. Chen L, Lian H, Huo R, et al. Uncertainty analysis in acoustics: Perturbation methods and isogeometric boundary element methods. Engineering with Computers. 2024; 40(6): 3875–3900. doi: 10.1007/s00366-024-02018-7
8. Zhou Z, Gao Y, Cheng Y, et al. Uncertainty Quantification of Vibroacoustics with Deep Neural Networks and Catmull–Clark Subdivision Surfaces. Shock and Vibration. 2024; 2024(1): 7926619. doi: 10.1155/2024/7926619
9. Zhang Z, Valeo C. Fuzzy-based input method for uncertainty quantification in a deterministic model comparison with ChatGPT for peak flow prediction. Journal of Hydrology X. 2025; 28–29: 100208. doi: 10.1016/j.hydroa.2025.100208
10. Sudhir Kumar A, Dhua S. Dynamic analysis of piezoelectric beams under fuzzy initial conditions: A comparative study. Journal of Vibration and Control. 2026; 10775463261430643. doi: 10.1177/10775463261430643
11. Ihlenburg F. Finite Element Analysis of Acoustic Scattering. Springer; 1998.
12. Bonnet M. Boundary Integral Equation Methods for Solids and Fluids. Wiley; 1999.
13. Fishman A. Monte Carlo: Concepts, Algorithms, and Applications. Springer; 1996.
14. Tuan NH, Huynh LX, Anh PH. A fuzzy finite element algorithm based on response surface method for free vibration analysis of structure. Vietnam Journal of Mechanics. 2015; 37(1): 17–27. doi: 10.15625/0866-7136/37/1/3923
15. Sobol′ IM. Global sensitivity indices for nonlinear mathematical models and their Monte Carlo estimates. Mathematics and Computers in Simulation. 2001; 55(1–3): 271–280. doi: 10.1016/S0378-4754(00)00270-6
16. Saltelli A, Ratto M, Tarantola S, et al. Sensitivity Analysis in Practice: A Guide to Assessing Scientific Models. Wiley; 2004.
17. Rao SS. Mechanical Vibrations. Pearson; 2017.
18. de Silva CW. Vibration: Fundamentals and Practice. CRC Press; 2007.
19. Blatman G, Sudret B. Adaptive sparse polynomial chaos expansion based on least angle regression. Journal of Computational Physics. 2011; 230(6): 2345–2367. doi: 10.1016/j.jcp.2010.12.021
20. Sudret B. Global sensitivity analysis using polynomial chaos expansions. Reliability Engineering & System Safety. 2008; 93(7): 964–979. doi: 10.1016/j.ress.2007.04.002
21. Bendat JS, Piersol AG. Random Data: Analysis and Measurement Procedures. Wiley; 2010.
22. Tieng SM, Yan AC. Investigation of mixed convection about a rotating sphere by holographic interferometry. Journal of Thermophysics and Heat Transfer. 1992; 6(4): 727–732. doi: 10.2514/3.11558
23. Bovik AC. The Essential Guide to Signal Processing. Elsevier Academic Press; 2009.
24. Ljung L. System Identification: Theory for the User. Prentice Hall; 1999.
25. Wang C, Qiu Z, Li Y. Hybrid uncertainty propagation of coupled structural–acoustic system with large fuzzy and interval parameters. Applied Acoustics. 2016; 102: 62–70. doi: 10.1016/j.apacoust.2015.09.006

26. Xia B, Yu D, Liu J. Interval and subinterval perturbation methods for a structural-acoustic system with interval parameters. Journal of Fluids and Structures. 2013; 38: 146–163. doi: 10.1016/j.jfluidstructs.2012.12.003
27. Yogeesh N. Fuzzy Logic Modelling of Nonlinear Metamaterials. In: Advances in Wireless Technologies and Telecommunication. IGI Global; 2023. pp. 230–269. doi: 10.4018/978-1-6684-8287-2.ch010
28. He CH, Cui Y, He JH, et al. Nonlinear dynamics in MEMS systems: Overcoming pull-in challenges and exploring innovative solutions. Journal of Low Frequency Noise, Vibration and Active Control. 2026; 45(1): 296–328. doi: 10.1177/14613484251385061
29. He JH, Ma J, Alsolami AA, et al. Variational approach to micro-electro-mechanical systems. Facta Universitatis, Series: Mechanical Engineering. 2025; 23(4): 649. doi: 10.22190/FUME250528023H
30. Saltelli A, Annoni P, Azzini I, et al. Variance based sensitivity analysis of model output. Design and estimator for the total sensitivity index. Computer Physics Communications. 2010; 181(2): 259–270. doi: 10.1016/j.cpc.2009.09.018
31. McKay MD, Beckman RJ, Conover WJ. Comparison of Three Methods for Selecting Values of Input Variables in the Analysis of Output from a Computer Code. Technometrics. 1979; 21(2): 239–245. doi: 10.1080/00401706.1979.10489755
32. Sobol' IM. On the distribution of points in a cube and the approximate evaluation of integrals. USSR Computational Mathematics and Mathematical Physics. 1967; 7(4): 86–112. doi: 10.1016/0041-5553(67)90144-9